

# Photonic Generation of Phase-Coded Microwave Signal With Large Frequency Tunability

Ze Li, *Student Member, IEEE*, Wangzhe Li, *Student Member, IEEE*, Hao Chi, Xianmin Zhang, and Jianping Yao, *Senior Member, IEEE*

**Abstract**—A photonic approach to realizing phase-coded microwave signal generation with large frequency tunability is proposed and demonstrated. Two coherent optical wavelengths are generated based on external modulation by biasing a Mach–Zehnder modulator (MZM) at the minimum transmission point to generate  $\pm 1$ -order sidebands while suppressing the optical carrier. The two  $\pm 1$ -order sidebands are then sent to a fiber Sagnac interferometer (SI) incorporating an optical phase modulator (PM) and a broadband flat-top fiber Bragg grating (FBG), with one of the sidebands being phase modulated at the PM. A frequency tunable phase-coded microwave signal is generated by beating the two sidebands at a photodetector (PD). The proposed technique is experimentally investigated. The generation of a frequency tunable phase-coded microwave signal at 22 and 27 GHz is demonstrated.

**Index Terms**—Microwave signal generation, phase coding, radar pulse compression.

## I. INTRODUCTION

IN modern radar systems, pulse compression has been widely used to increase the range resolution [1]. Usually, pulse compression is implemented in a radar receiver by compressing a frequency-chirped or phase-coded pulse using a matched filter. Chirped or phase-coded pulses can be generated in the electrical domain using electronic circuitry. The main limitation of the electrical techniques is the small time-bandwidth product (TBWP), which limits the pulse compression ratio. A solution to generate a chirped or phase-coded pulse with a large TBWP is to use photonics techniques [2]–[8]. In [2], [3], a chirped or phase-coded microwave pulse was generated using a pulse shaping system in which a spatial light modulator (SLM) was employed. However, since an SLM-based system involves the use of free-space optics, the system is usually bulky and lossy. A chirped or phase-coded microwave pulse can also be generated using an all-fiber-based system. In [4],

a linearly chirped microwave pulse was generated by beating two linearly chirped optical pulses with different chirp rates at a photodetector (PD). In [5], a high-frequency chirped electrical pulse was generated based on optical spectral shaping and frequency-to-time mapping in a dispersive element. In [6], a technique to generate a phase-coded microwave pulse was demonstrated. However, the stability of the system was poor due to the use of a Mach–Zehnder interferometer [6]. To achieve a stable operation, a technique based on a photonic microwave delay-line filter was proposed [7]. The major limitation of the approach in [7] is the narrow bandwidth of the delay-line filter, which limits the bandwidth of the generated pulse. A technique to generate a phase-coded microwave pulse with a large bandwidth was recently demonstrated using a polarization modulator (PoM) [8]. The major limitation of the technique is that the microwave frequency is not tunable as the orthogonality of the two light waves to the PoM is dependent on the wavelength spacing.

In this letter, we propose and demonstrate a novel approach to realizing phase-coded microwave signal generation with large frequency tunability. In the approach, two coherent optical wavelengths are generated based on external modulation by biasing a Mach–Zehnder modulator (MZM) at the minimum transmission point (MITP) to generate  $\pm 1$ -order sidebands while suppressing the optical carrier. The two sidebands are then sent to a fiber Sagnac interferometer (SI), incorporating a phase modulator (PM) and a broadband flat-top fiber Bragg grating (FBG), with one of the sidebands being phase modulated at the PM. By beating the two sidebands at a PD, a phase-coded microwave signal is generated. The frequency of the phase-coded microwave signal can be tuned by tuning the frequency of the microwave driving signal. The proposed technique is experimentally investigated. A phase-coded microwave signal at 22 and 27 GHz is generated.

## II. PRINCIPLE

The schematic of the proposed system is shown in Fig. 1. A CW light wave from a tunable laser source (TLS) is sent to an MZM through a polarization controller (PC1). A sinusoidal microwave driving signal is applied to the MZM, which is biased at the MITP to generate two  $\pm 1$ -order sidebands while suppressing the optical carrier. The two sidebands are then sent to an SI through PC2. The SI consists of a 3-dB optical coupler (OC), an optical isolator (OI), an FBG and a PM. The bidirectional operation of the PM is employed. Due to the velocity match in the PM, the light wave that is copropagating with the microwave signal is efficiently modulated. When the light wave

Manuscript received October 21, 2010; revised February 06, 2011; accepted March 16, 2011. Date of publication March 24, 2011; date of current version May 13, 2011. This work was supported by the Natural Sciences and Engineering Research Council of Canada (NSERC). The work of Z. Li was supported by a scholarship from the China Scholarship Council.

Z. Li is with the Microwave Photonics Research Laboratory, School of Information Technology and Engineering, University of Ottawa, Ottawa, ON K1N 6N5, Canada, and also with the Department of Information Science and Electronic Engineering, Zhejiang University, Hangzhou, 310027 China.

W. Li and J. Yao are with the Microwave Photonics Research Laboratory, School of Information Technology and Engineering, University of Ottawa, Ottawa, ON K1N 6N5, Canada (e-mail: jpyao@site.uOttawa.ca).

H. Chi and X. Zhang are with the Department of Information Science and Electronic Engineering, Zhejiang University, Hangzhou, 310027 China.

Color versions of one or more of the figures in this letter are available online at <http://ieeexplore.ieee.org>.

Digital Object Identifier 10.1109/LPT.2011.2132121

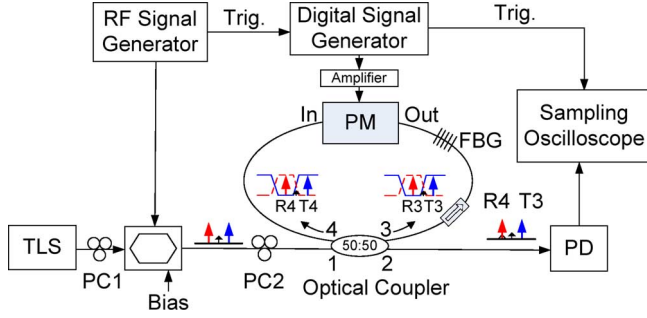


Fig. 1. Schematic of the proposed phase-coding system. Trig.: trigger.

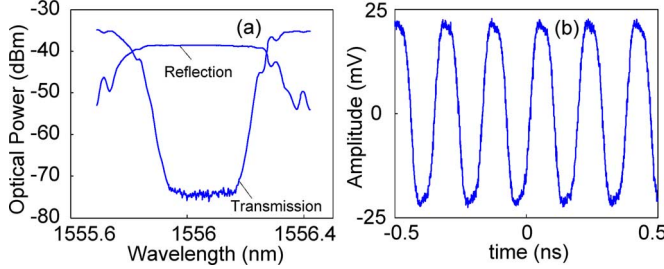


Fig. 2. (a) Transmission and reflection spectra of the FBG. (b) Binary phase-coding signal at the output of the amplifier. To perform the measurement, the power of the modulation signal is attenuated.

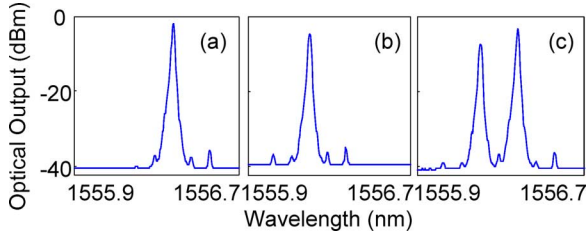


Fig. 3. Optical spectra of the  $\pm 1$ -order optical sidebands. (a) Transmitted 1-order sideband. (b) Reflected  $-1$ -order sideband. (c) Combined two sidebands at the output of the SI.

is counterpropagating with the microwave signal, it is inefficiently modulated due to the velocity mismatch, with a modulation depth that is 15 dB lower.

As shown in Fig. 1, the two sidebands from the MZM are directed to port 1 of the OC and are split into two branches (port 3 and port 4). The sidebands from port 3 would pass through the OI and enter the FBG. The wavelength of the  $-1$ -order sideband, R3, falls in the reflection band of the FBG, and is reflected by the FBG. Due to the high isolation ( $> 40$  dB) of the OI, R3 is blocked. The  $+1$ -order sideband, T3, would pass through the FBG and enter the PM from the output port. Due to the low modulation depth, T3 is not modulated. Similarly, the sidebands from port 4 enter the PM from the input port and are modulated by the phase coding signal. The wavelength of the  $-1$ -order sideband, R4, falls in the reflection band of the FBG and will be reflected back to part 4 through the PM. The  $+1$ -order sideband, T4, would pass through the FBG but be blocked by the OI. Therefore, at the output of the OC (port 2), there are two wavelengths, the  $-1$ -order sideband with phase modulation and the  $+1$ -order sideband with no phase modulation. A phase-coded microwave signal is thus obtained by beating R4 and T3 at a PD.

Assume a binary phase-coding signal  $s(t)$  with amplitude of  $V_p$  is applied to the PM. The two sidebands at the output of the SI could be expressed as

$$E_{T3}(t) = \exp[j(\omega_0 - \omega_m)t] \quad (1)$$

and

$$E_{R4}(t) = \exp\left\{j\left[(\omega_0 + \omega_m)t + \pi\left(\frac{V_p}{V_\pi}\right) \cdot s(t)\right]\right\} \quad (2)$$

where  $\omega_0$  and  $\omega_m$  are the angular frequencies of the optical carrier and the microwave driving signal, and  $V_\pi$  is the half-wave voltage of the PM. Thus, the phase-coded microwave signal at the output of the PD is

$$i(t) = R \cdot E_{R4} E_{T3}^* = R \cdot \exp\left\{j\left[2\omega_m t + \pi\left(\frac{V_p}{V_\pi}\right) \cdot s(t)\right]\right\} \quad (3)$$

where  $R$  is the responsivity of the PD and  $*$  denotes phase conjugation. As can be seen from (3), a frequency-doubled phase-coded microwave signal is obtained.

### III. EXPERIMENTAL RESULTS

An experiment based on the setup shown in Fig. 1 is performed. A broadband flat-top FBG is fabricated. The transmission and reflection spectra of the FBG are shown in Fig. 2(a). To ensure large frequency tunability, the wavelength of the optical carrier is placed at the right edge of the FBG. An 11-GHz microwave signal from a signal generator (Agilent E8254A) with a power of 22 dBm is applied to the MZM which is biased at the MITP. An 11 Gb/s digital signal from a bit error rate tester (BERT) is amplified and then applied to the PM to achieve phase coding. The binary phase-coding signal at the output of the amplifier is shown in Fig. 2(b). The phase-coded microwave signal is generated at the output of a PD, and monitored by a sampling oscilloscope (Agilent 86100C).

Fig. 3 shows the optical spectra of the  $\pm 1$ -order optical sidebands measured by an optical spectrum analyzer. The transmitted  $+1$ -order sideband in Fig. 3(a) is detected at the input port of the PM by disconnecting it from port 4 of the OC. The reflected  $-1$ -order sideband in Fig. 3(b) is detected at port 2 of the OC by disconnecting port 3 and the OI. The combined two sidebands in Fig. 3(c) are measured at the output of the SI. As can be seen, the isolation between the two optical sidebands is larger than 30 dB and the power of the optical carrier is also 30 dB lower than those of the two sidebands.

Fig. 4(a) shows the generated 22-GHz microwave signal at the output of the PD without phase coding. The generated 22 GHz phase-coded microwave is shown in Fig. 4(b). In the experiment, the power  $P$  of the phase-coding signal from the BERT is about 24 dBm. Thus, the amplitude  $V_p$  of the modulating signal is calculated to be 3.54 V based on  $V_p = \sqrt{P Z_m}$  for a square wave, where the input impedance of the PM,  $Z_m$ , is 50  $\Omega$  [8]. As the half-wave voltage of the PM is about 11 V, the phase shifts corresponding to “1” and “ $-1$ ” are calculated to be  $58^\circ$  and  $-58^\circ$  according to (3). Therefore, the phase shift difference between “1” and “ $-1$ ” is around  $116^\circ$ . Fig. 4(c)

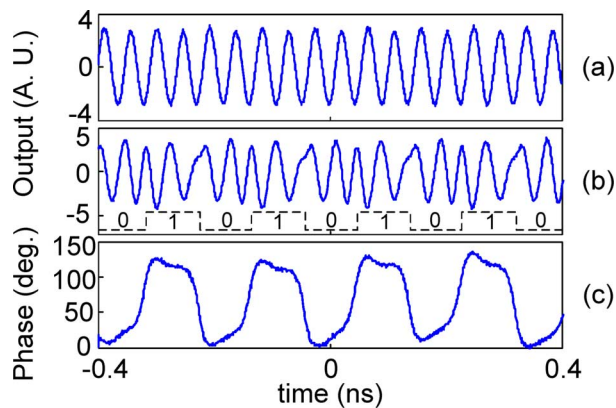


Fig. 4. (a) Generated 22-GHz microwave signal without phase coding. (b) Phase-coded 22-GHz microwave signal. (c) Recovered phase information from the microwave signal in (b). deg.: degree.

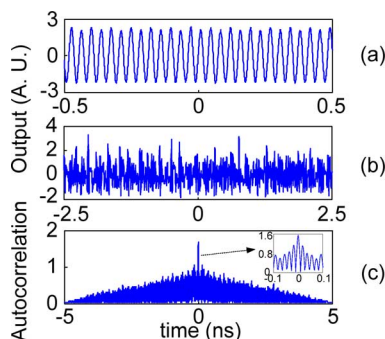


Fig. 5. (a) Generated 27-GHz microwave signal without phase coding. (b) Measured 27-GHz phase-coded signal. (c) Calculated autocorrelation between the original phase-coded microwave signal and the phase-coded signal with a white Gaussian noise.

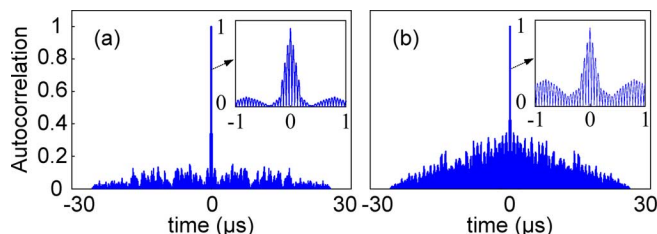


Fig. 6. Calculated autocorrelation results for different phase shift difference. (a)  $180^\circ$ ; (b)  $120^\circ$ .

shows the phase information of the phase-coded signal recovered using the Hilbert transform. As can be seen, the maximum phase shift difference between “1” and “-1” is  $125^\circ$ , which agrees well with the theoretical value.

To demonstrate the frequency tunability, the frequency of the microwave driving signal is tuned to 13.5 GHz. Fig. 5(a) shows the generated 27-GHz microwave signal. Then, a 13.5-Gb/s pseudorandom bit sequence (PRBS) with a length of 128 bits and a power of 24 dBm is used as the phase-coding signal to demonstrate the pulse compression capability. Fig. 5(b) shows the generated phase-coded signal with 5-ns time duration. The TBWP is calculated to be 67.5. An additive white Gaussian noise (AWGN) is added to demonstrate the robustness of the pulse compression technique to noise. The signal with an AWGN has a signal-to-noise ratio (SNR) as low as 0 dB. Fig. 5(c) shows the correlation between the original phase-coded microwave signal (as a reference) and the phase-coded signal with an AWGN. As can be seen, the auto-

correlation peak has a 3-dB bandwidth of 74 ps. A compression ratio of 67.6 is achieved.

#### IV. DISCUSSION AND CONCLUSION

From Fig. 5(c), a small peak-to-sidelobe ratio (PSR) is observed. This is resulted from the small phase shift of the generated phase-coded signal due to the high half-wave voltage of the PM. To evaluate the dependence of the PSR on the phase shift, a simulation is performed. A 128-bit random binary signal is generated and used as the phase-coding signal. The microwave carrier frequency is set at 10 MHz and the bit rate of the phase-coding signal is at 5 Mb/s. Fig. 6(a) shows the autocorrelation when the phase shift difference between “+1” and “-1” is  $180^\circ$ . It can be seen that the PSR is about 6.7. Then, we reduce the phase shift difference to  $120^\circ$ . The autocorrelation is shown in Fig. 6(b). It is seen that the PSR is decreased to 2.7. If a PM with a smaller half-wave voltage is used, the PSR of the generated pulse could be improved.

The minimum frequency of the microwave signal is limited by the transition bandwidth of the FBG, which can be as small as 0.1 nm, corresponding to a smallest frequency of 12.5 GHz. The maximum frequency is limited by the bandwidth of the PD. Considering that a PD with a bandwidth up to 100 GHz is commercially available, the tunable range can be from 12.5 to 100 GHz.

In the experiment, a good short-term stability (about 3 minutes) is observed. The long-term stability is relatively poor, due to the bias drift of the MZM and the slow change of the Sagnac-loop length. A solution to the problem is to integrate the system using a monolithically photonic integrated circuit.

In conclusion, we have proposed and demonstrated a novel approach to generating phase-coded microwave signals with large frequency tunability. The key module in the system is the SI incorporating a PM and an FBG, which ensures the generation of two optical sidebands with one being phase modulated. The beating of the two sidebands at a PD would generate a phase-coded microwave signal. An experiment was performed. The generation of a phase-coded microwave signal at 22 and 27 GHz was demonstrated.

#### REFERENCES

- [1] M. I. Skolnik, *Introduction to Radar*. New York: McGraw-Hill, 1962.
- [2] J. D. McKinney, D. E. Leaird, and A. M. Weiner, “Millimeter-wave arbitrary waveform generation with a direct space-to-time pulse shaper,” *Opt. Lett.*, vol. 27, no. 5, pp. 1345–1347, Aug. 2002.
- [3] J. Chou, Y. Han, and B. Jalali, “Adaptive RF-photonics arbitrary waveform generator,” *IEEE Photon. Technol. Lett.*, vol. 15, no. 4, pp. 581–583, Apr. 2003.
- [4] A. Zeitouny, S. Stepanov, O. Levinson, and M. Horowitz, “Optical generation of linearly chirped microwave pulses using fiber Bragg gratings,” *IEEE Photon. Technol. Lett.*, vol. 17, no. 3, pp. 660–662, Mar. 2005.
- [5] C. Wang and J. P. Yao, “Chirped microwave pulse compression using a photonic microwave filter with a nonlinear phase response,” *IEEE Trans. Microw. Theory Tech.*, vol. 57, no. 2, pp. 496–504, Feb. 2009.
- [6] H. Chi and J. P. Yao, “An approach to photonic generation of high-frequency phase-coded RF pulses,” *IEEE Photon. Technol. Lett.*, vol. 19, no. 10, pp. 768–770, May 15, 2007.
- [7] Y. Dai and J. P. Yao, “Microwave pulse phase encoding using a photonic microwave delay-line filter,” *Opt. Lett.*, vol. 32, no. 24, pp. 3486–3488, Dec. 2007.
- [8] H. Chi and J. P. Yao, “Photonic generation of phase-coded millimeter-wave signal using a polarization modulator,” *IEEE Microw. Wireless Compon. Lett.*, vol. 18, no. 5, pp. 371–373, May 2008.